Article

Molecular Spatiomics by Proximity Labeling

Myeong-Gyun Kang and Hyun-Woo Rhee*

Cite This: *Acc. Chem. Res.* 2022, 55, 1411−1422

Read Online

ACCESS | Metrics & More | Article Recommendations

CONSPECTUS: Proximity labeling can be defined as an enzymatic "in-cell" chemical reaction that catalyzes the proximity-dependent modification of biomolecules in live cells. Since the modified proteins can be isolated and identified via mass spectrometry, this method has been successfully utilized for the characterization of local proteomes such as the sub-mitochondrial proteome and the proteome at membrane contact sites, or spatiotemporal interactome information in live cells, which are not "accessible" via conventional methods. Currently, proximity labeling techniques can be applied not only for local proteome mapping but also for profiling local RNA and DNA, in addition to showing great potential for elucidating spatial cell−cell interaction networks in live animal models. We believe that proximity labeling has emerged as an essential tool in "spatiomics," that is, for the extraction of spatially distributed biological information in a cell or organism.

Proximity labeling is a multidisciplinary chemical technique. For a decade, we and other groups have engineered it for multiple applications based on the modulation of enzyme chemistry, chemical probe design, and mass analysis techniques that enable superior mapping results. The technique has been adopted in biology and chemistry. This "in-cell" reaction has been widely adopted by biologists who modified it into an in vivo reaction in animal models. In our laboratory, we conducted in vivo proximity labeling reactions in mouse models and could successfully obtain the liver-specific secretome and muscle-specific mitochondrial matrix proteome. We expect that proximity reaction can further contribute to revealing tissue-specific localized molecular information in live animal models.

Simultaneously, chemists have also adopted the concept and employed chemical "photocatalysts" as artificial enzymes to develop new proximity labeling reactions. Under light activation, photocatalysts can convert the precursor molecules to the reactive species via electron transfer or energy transfer and the reactive molecules can react with proximal biomolecules within a definite lifetime in an aqueous solution. To identify the modified biomolecules by proximity labeling, the modified biomolecules should be enriched after lysis and sequenced using sequencing tools. In this analysis step, the direct detection of modified residue(s) on the modified proteins or nucleic acids can be the proof of their labeling event by proximal enzymes or catalysts in the cell. In this Account, we introduce the basic concept of proximity labeling and the multidirectional advances in the development of this method. We believe that this Account may facilitate further utilization and modification of the method in both biological and chemical research communities, thereby revealing unknown spatially distributed molecular or cellular information or spatiome.
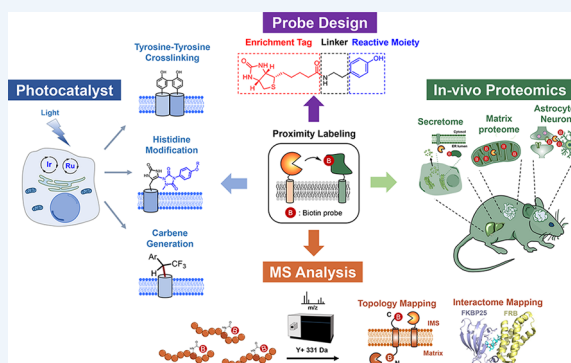
■ KEY REFERENCES

- Lee, S. Y.; Kang, M. G.; Shin, S.; Kwak, C.; Kwon, T.; Seo, J. K.; Kim, J. S.; Rhee, H. W. Architecture Mapping of the Inner Mitochondrial Membrane Proteome by Chemical Tools in Live Cells. *J. Am. Chem. Soc.* **2017**, *139*, 3651−3662.[1] *In this paper, desthiobiotin-phenol (DBP) was used for the direct mass detection of APEX-labeled peptides (Spot-ID). The membrane topology of 135 IMM proteins was revealed via Matrix-APEX2 and IMS-APEX2 with direct analysis of the DBP-labeled site.*

- Lee, S. Y.; Lee, H.; Lee, H. K.; Lee, S. W.; Ha, S. C.; Kwon, T.; Seo, J. K.; Lee, C.; Rhee, H. W. Proximity-Directed Labeling Reveals a New Rapamycin-Induced Hetero-dimer of FKBP25 and FRB in Live Cells. *ACS Cent. Sci.*

2016, *2*, 506−516.[2] *In this work, direct mass detection of biotin-labeled proteins by BioID (Spot-BioID) was first proposed. As a model experiment, FRB-BioID was used for identification of an unknown interacting target at the FRB domain that is induced by rapamycin. According to the Spot-BioID analysis results, FKBP25 exhibited highest biotinyla-*

Scheme 1. Comparison of Substrate Positions in the Crystal Structures of Ascorbate Peroxidase (APX, PDB ID: 1OAF) and Biotin Ligase (BirA, PDB ID: 2EWN)[a]
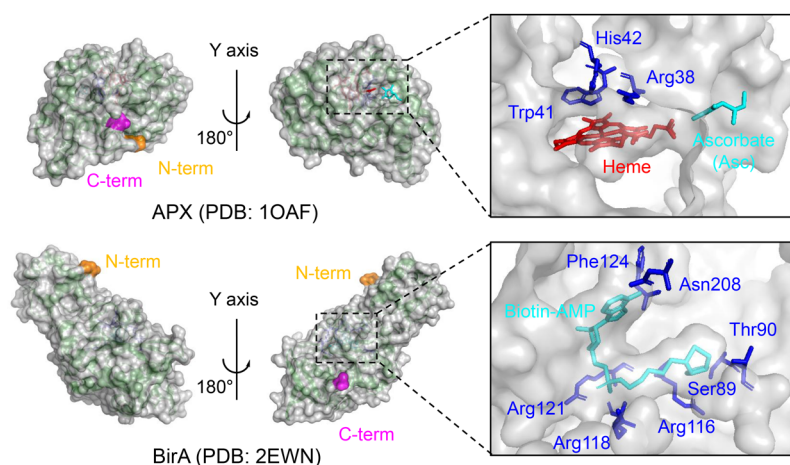
[a]Substrate molecules are colored in light blue.

tion by BioID, and the crystal structure of the FKBP25-rapamycin-FRB complex was successfully obtained.

- Kwak, C.; Shin, S.; Park, J. S.; Jung, M.; Nhung, T. T. M.; Kang, M. G.; Lee, C.; Kwon, T. H.; Park, S. K.; Mun, J. Y.; Kim, J. S.; Rhee, H. W. Contact-ID, a tool for profiling organelle contact sites, reveals regulatory proteins of mitochondrial-associated membrane formation. *Proc. Natl. Acad. Sci. U. S. A.* **2020**, *117*, 12109.[3] *In this work, a new split system of BioID (Contact-ID) was developed to identify the local proteome at contact sites between the ER and mitochondria, with 115 mitochondrial-associated membrane (MAM) proteins revealed by Spot-BioID analysis. Among these was FKBP8, a mitochondrial outer membrane protein involved in MAM formation and calcium transport.*

■ INTRODUCTION

Most proteins exert their effect via networks with other molecules. The identification of protein networks is essential for understanding cellular processes at the systems level. Co-immunoprecipitation and fractionation methods have contributed to revealing the spatial proteomic information. However, these methods may yield false results based on artificial protein interactions, as purification is performed on lysates wherein all subcellular microenvironments are completely disrupted, with artificial buffer conditions allowing artifactual protein−protein interactions. Proximity labeling (PL) is recognized as a useful tool for obtaining spatially distributed molecular localization information, dubbed "molecular spatiomics" in live cells.

PL can be defined as a spatially restricted enzymatic modification reaction on proximal biomolecules (e.g., protein, RNA, DNA). Since this modification reaction can occur via reactive probes conjugated with biotin or similar conjugates, the modified biomolecules can be enriched via streptavidin beads or related methods. Currently, various enzymatic reactions have been utilized for PL,[4] and we will highlight two enzymatic reactions, namely those catalyzed by peroxidases (APEX) and biotin ligases (BioID or TurboID), which are widely employed in biological research.

APEX is a peroxidase originally engineered from ascorbate peroxidase (APX),[5] which is expressed in the cytosol of plants.

The molecular weight of APEX is approximately 28 kDa, similar to the size of green fluorescent protein (GFP), which has been widely used for imaging various proteins of interest. APX reduces hydrogen peroxide (H_2O_2) via oxidation of aromatic molecules (e.g., ascorbic acid, phenol), thus playing a role in plant cell antioxidant protection. During this process, two electrons are sequentially extracted from two phenol substrates to the oxidized heme within the active site of APX, and phenolic compounds are turned to the phenoxyl radicals that can be coupled to the tyrosine residues of proximal proteins. As the half-life of phenoxyl radicals in aqueous solution is below 1 ms,[6] proximal proteins less than 20 nm away can be targeted by these radicals.[1,7] Engineered ascorbate peroxidase (APEX, APEX2) enzymes with enhanced catalytic activity relative to the wild-type enzyme have been engineered.[5,8]

It should be noted that variable chemical probes have been developed for APEX,[1,6,9−13] while there is currently no variation in the substrates for other PL enzymes such as biotin ligases (e.g., BioID/TurboID). The underlying reason lies within the crystal structure of APX. The heme binding pocket of APX is in a partially solvent-exposed position and the aromatic substrate binding site is located at the solvent-exposed edge of heme (Scheme 1)[14] as shown in other peroxidase structures including horseradish peroxidase (HRP),[5] which was initially used in the EMARS method.[15] Since phenoxyl radical generation occurs at the protein surface, APX and HRP have weak substrate specificity.[5] This property is beneficial for probe development with variable combinations of different enrichment handles, linker sizes, and aromatic moieties for the peroxidase-mediated PL reaction.

Another enzyme widely used in PL is biotin ligase (e.g., BioID or TurboID). Both BioID and TurboID are engineered derivatives of *E. coli* biotin ligase (BirA),[16] and the molecular weight of these enzymes is approximately 35 kDa, which is higher than that of APEX. These enzymes generate biotin-AMP ester (biotin-AMP) through a coupling reaction between biotin and ATP within the enzyme active site. Since biotin-AMP is an electrophilic activated ester, it reacts with lysine residues on proximal proteins when released from the active site. Originally, wild-type BirA was considered to catalyze only a very specific biotinylation reaction with one substrate protein, namely biotin carboxyl carrier protein (BCCP) in *E. coli*. In this reaction,
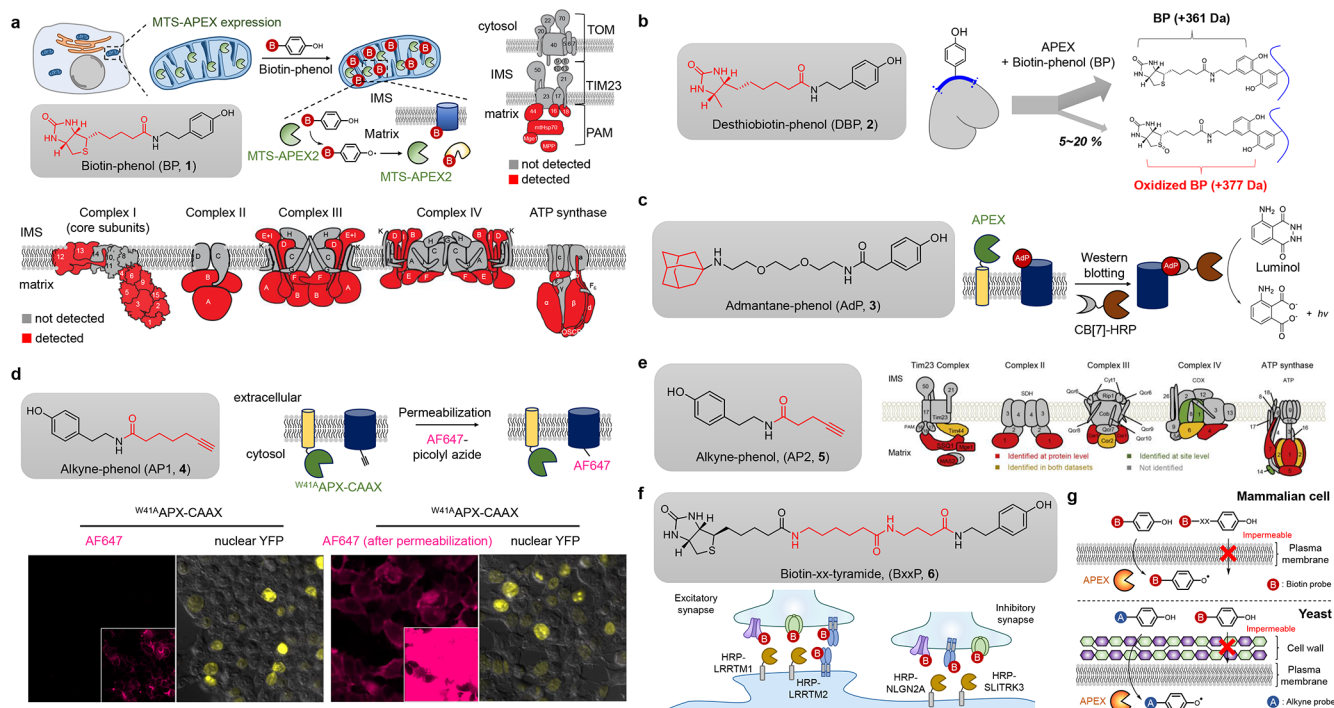
Figure 1. Chemical variation in enrichment handle and linker of APEX/HRP probes (a) APEX labeling with BP was performed for mitochondrial matrix proteome characterization. Detected OXPHOS and TOM-TIM23 subunits by matrix-APEX are colored in red. Reprinted with permission from ref 6. Copyright 2013 AAAS. (b) DBP was synthesized to avoid oxidation, enhancing signal intensity in LC-MS/MS. (c) Detection of AdP labeled proteins using Western blotting with CB[7]-HRP. (d) Determination of alkyne phenoxyl radical permeability through cell membranes using APX-CAAX, with APX facing the cytoplasm. Reprinted with permission from ref 6. Copyright 2013 AAAS. (e) Mitochondrial matrix proteome mapping in yeast using cell-permeable alkyne phenol. Reprinted with permission from ref 10. Copyright 2020 Elsevier. (f) Strategy for specific mapping of the synaptic cleft with membrane impermeable BxxP. (g) Scheme of the permeability of probes to membrane in mammalian cells and yeast.

biotin-AMP is kept within the active site by a binding loop (116−124 aa). However, biotin-AMP can be released into the solution by the R118G promiscuous mutant BirA (pBirA or BioID).[17,18] It can then react with the primary amine group of lysine residues on proximal proteins.[19] TurboID is a kinetically engineered version of BirA obtained via yeast display.[20] Although biotin-AMP has a half-life of several minutes in aqueous solution,[21−23] BioID and TurboID labeling provide a comparable spatial resolution to APEX, possibly due to the short half-life of biotin-AMP within protein-rich environments, since lysine is the abundant amino acid residue on protein surfaces.[24] However, as previously mentioned, there is only one report (i.e., SS-Biotin)[25] on the use of biotin analogs in PL via BioID or TurboID[26] because biotin has high selectivity for the binding pocket of BirA, as shown in the crystal structure[17] (Scheme 1).

Both APEX and BioID/TurboID generate biotin-modified proteins, which require mass spectrometry analysis after streptavidin enrichment. Since conventional mass analysis approaches for the detection of unmodified peptides of an enriched proteome can provide only indirect information of the biotin-modified proteome, we and others found that direct mass detection of the modified region (e.g., modified site or modified peptides) can provide more accurate information for the local proteome as well as structural details of the modified sites.[1,27] Overall, we consider PL a multidisciplinary method, which combines synthetic chemistry (e.g., probe and catalyst design), biochemistry (e.g., protein engineering), and analytical chemistry (e.g., mass analysis). In this Account, we provide an overview of our recent progress on PL in synthetic and analytical chemistry. We also review the latest progress in biology-oriented

in vivo applications of PL and chemistry-oriented advances in photocatalyst-mediated PL development. Lastly, we will outline future perspectives for PL in biological research.

CHEMICAL DESIGN FOR PL

In the first use of APEX-based PL in 2013, biotin-phenol (BP, **1**) was prepared for mapping the mitochondrial matrix proteome (Figure 1a).[6] Within BP, the phenol part of tyramine is the only chemical moiety to react with peroxidase, and biotin is added for streptavidin enrichment prior to LC-MS/MS analysis. BP has moderate cell membrane permeability. Preincubation of BP for 30 min, and 1 min H_2O_2 addition to matrix-APEX-expressing cell line generated nearly saturated biotin-labeled signals within mitochondria, indicating that BP can penetrate multiple membranes from media into the mitochondrial matrix. Mass spectrum analysis yielded 495 mitochondrial matrix proteins following the in situ biotinylation reaction with matrix-targeting APEX (matrix-APEX) and LC-MS/MS profiling after streptavidin enrichment. Our results were in agreement with matrix-side localized subunits of OXPHOS and TIM-TOM import complexes (Figure 1a). Among the 495 proteins, PPOX and PNPT1, previously known as mitochondrial intermembrane space (IMS) proteins, were also labeled via matrix-APEX, and confirmed to localize within the mitochondrial matrix through APEX-based electron microscopy (EM) imaging.[6] After this publication, various subcellular spaces, including the IMS,[28] endoplasmic reticulum (ER) and plasma membrane (PM) junction,[29] stress granule,[30] or the GPCR interactome,[31] were studied using BP (**1**).
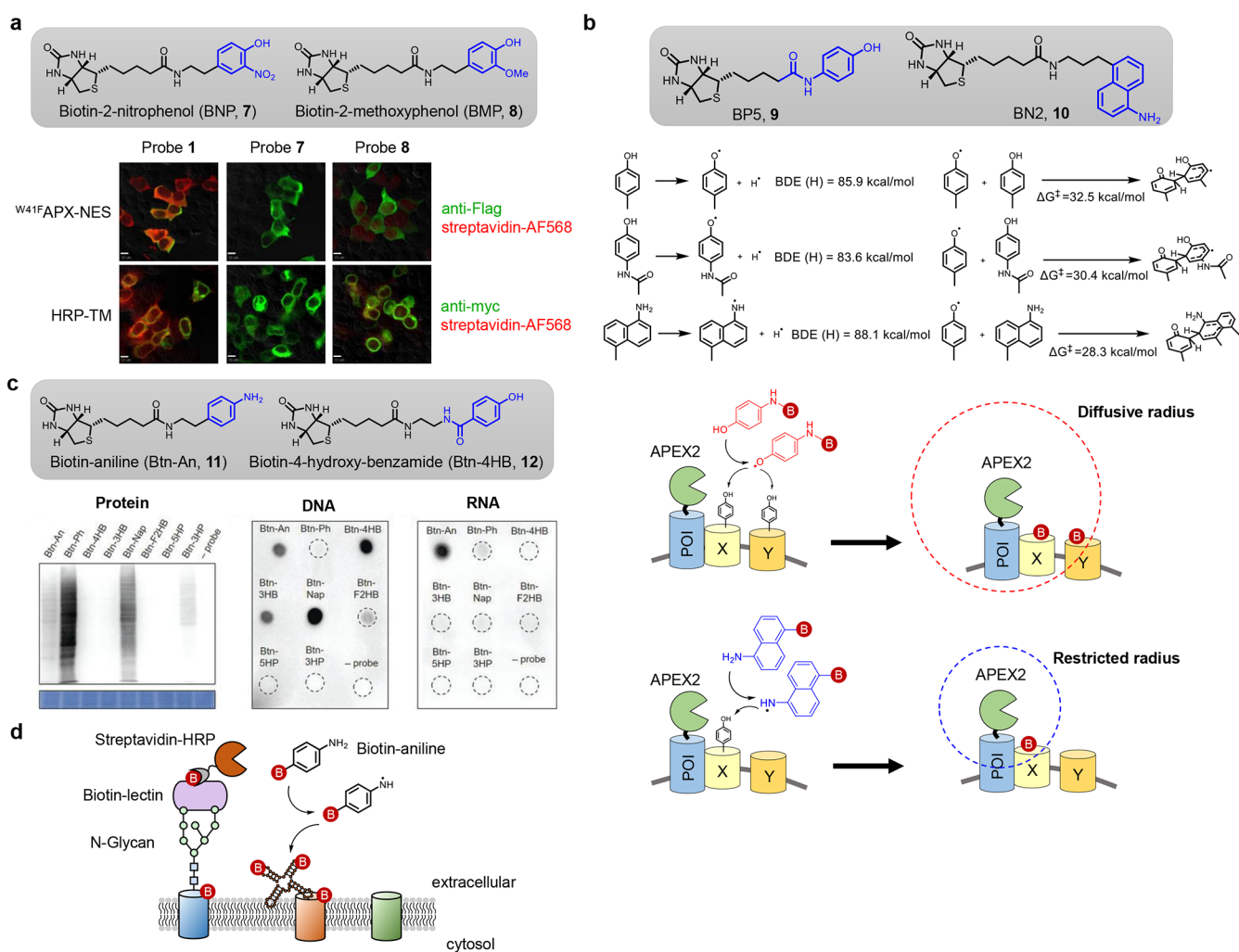
Figure 2. Chemical variation in reactive moiety of APEX/HRP probes. (a) Reactivity of BNP and BMP toward APX and HRP. Reprinted with permission from ref 6. Copyright 2013 AAAS. (b) Scheme of highly selective PL with BP5 and BN2 for mapping the EGFR interactome upon EGF stimulation and the ILK−PINCH-PARVIN-RSU1 protein complex in the cytosol, respectively. The BDE and reaction barrier for BP5 and BN2 were evaluated. (c) Screening the BP derivatives for protein, DNA, and RNA labeling. Reprinted with permission from ref 13. Copyright 2019 Wiley. (d) Scheme of the glycoRNA labeling on the cell surface using Btn-An.

Since biotin has strong binding affinity toward streptavidin $(K_a = 4 \times 10^{14}\ M^{-1})$,[1] BP-labeled proteins can be isolated using streptavidin beads. However, we realized that such high affinity might hamper the recovery of biotinylated peptides from the bead. We also observed that the thioether group of biotin is easily oxidized to sulfoxide or sulfone during the radical-generating APEX reaction, which results in splitting modified peptides to the nonoxidized and oxidized population. Thus, we developed desthiobiotin-phenol (DBP, **2**) which contains desthiobiotin, a sulfur-free biotin analogue, as an enrichment handle. While DBP shows a similar reactivity to the protein when it is converted to the phenoxyl radical state as BP,[1] DBP has no sulfur oxidation issue and binds less tightly to streptavidin $(K_a = 1 \times 10^{13}\ M^{-1})$,[1] resulting in higher recovery of DBP-modified peptides from streptavidin beads after the APEX reaction (Figure 1b). Using DBP, we could obtain more mass spectra of APEX-labeled peptides, which is beneficial for characterizing the membrane topology of labeled membrane proteins.[1]

It should be noted that another chemical enrichment handle, admantane, which has high binding affinity $(K_a > 1.0 \times 10^{13}$

$M^{-1})$ with the host molecule, cucurbit[7]uril (CB7),[9] can be utilized for APEX labeling. Through collaboration with Dr. Kimoon Kim's research group, we found that adamantane-phenol (AdP, **3**) reacts with APEX in live cells (Figure 1c) and AdP-modified proteins were detected by Western blotting with CB7-conjugated HRP. Since admantane-modified protein can be enriched with CB7-conjugated beads,[32] this method may be useful for the orthogonal enrichment of APEX-labeled proteins, while almost all other PL methods are based on the biotin-modification and streptavidin bead enrichment, which have a potential issue in samples with high expression levels of endogenous biotinylated proteins.[33]

Another direction of APEX labeling is controlling membrane permeability of the chemical probe. While BP has moderate membrane permeability and is widely utilized in various mammalian cell experiments; however, it is not optimal for complexed membrane structures such as fruit fly,[34] Caeno-rhabditis elegans,[35] and yeast.[10] To improve the membrane permeability of BP, detergent pretreatment in fruit fly, bus-8 gene knock-down for reducing cuticle integrity in C. elegans, and zymolyase incubation for cell wall removal in yeast[36] have been
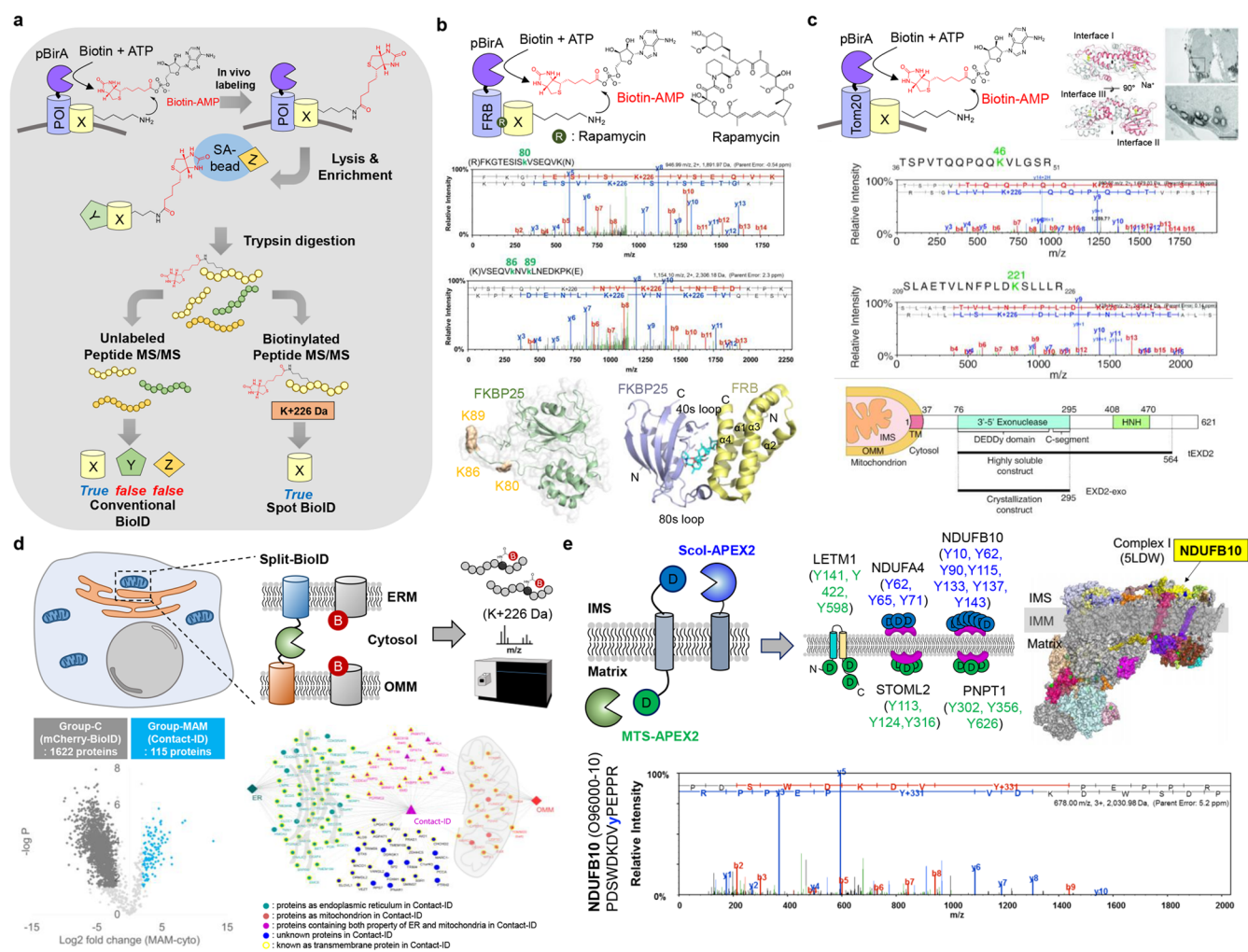
Figure 3. Direct mass analysis of PL-modified residues. (a) Schematic representation of LC-MS/MS sample preparation of the Spot-BioID. (b) Identification of FRB interaction partners under rapamycin treatment using Spot-BioID. Labeled sites are highlighted in the crystal structure of FKBP25 (PDB: 2MPH), and the FKBP25-rapamycin-FRB crystal structure is shown with a ribbon diagram (PDB: 5GPG). Reprinted with permission from ref 2. Copyright 2016 American Chemical Society. (c) Localization of EXD2 at the outer membrane of mitochondria was revealed via crystal structure (PDB: 6K17) and APEX-EM. Reprinted with permission from ref 41. Copyright 2019 Oxford University Press. (d) Overview of the Contact-ID method for mapping contact sites between mitochondria and ER. (e) Topology of the mitochondrial inner membrane proteins was revealed via Spot-ID. Reprinted with permission from ref 1. Copyright 2017 American Chemical Society.

performed even though these permeabilization steps may perturb the physiology to some extent. Thus, alkyne-phenol generated as an alkyne is a small lipophilic functional group that can be enriched via the click reaction,[6,10] exhibiting greater membrane permeability than biotin.[10] First, alkyne-phenol (AP1, **4**) was tested to assess whether the phenoxyl radical can permeate cell membranes.[6] The plasma membrane-targeted [W41A]APX (enhanced activity APX mutant)-CAAX reacted with alkyne-phenol, and almost no signal was detected without permeabilization prior to the click reaction (Figure 1d). These results indicate that alkyne-phenol is membrane-permeable, while the alkyne-phenoxyl radical is not. Utilizing this favorable cell membrane permeability of alkyne-phenol (AP2, **5**), the yeast mitochondrial matrix proteome was successfully characterized via mitochondrial matrix-targeted Su9-APEX2 (Figure 1e).[10]

Like the enrichment tag, linker size also has tremendous influence on membrane permeability (Figure 1g). A non-membrane-permeable probe can be useful for cell surface proteome-specific labeling within neurons. For cell surface labeling, peroxidase should be trafficked via the protein secretory

pathway (e.g., ER and Golgi apparatus). Consequently, membrane-permeable BP can react with cell surface-localized peroxidase as well as peroxidases remaining in ER and Golgi, limiting cell surface specificity. Therefore, biotin-xx-phenol (BxxP, **6**; x means hexanoyl) was used for mapping local proteomes in the excitatory and inhibitory synaptic cleft of neurons (Figure 1f).[11] Using BxxP and horseradish peroxidase (HRP) with excitatory synapse (LRRTM1 and LRRTM2) and inhibitory synapse-specific anchoring (NLGN2A and SLITRK3) proteins, 199 excitatory and 42 inhibitory synaptic cleft proteins were identified with high specificity (>89%) and high coverage (>69% and >46%, respectively). Notably, HRP was employed due to its robust enzymatic peroxidase reaction relative to APEX under oxidative conditions, as seen throughout the secretory pathway (e.g., ER, Golgi lumen, and cell surface).

Another important advance in chemical designs for APEX labeling is the modification of the reactive moiety. Chemical modification of the APEX probe aromatic moiety can regulate its labeling radius and reactivity to biomolecules. In the original work of APEX, we tested whether BP modification with an

electron-withdrawing group (EWG) or electron-donating group (EDG) can influence labeling activity. We generated biotin-2-nitrophenol (BNP, 7) and biotin-2-methoxyphenol (BMP, 8), both having an ortho modification of a nitro (EWG) and methoxy (EDG) group that can destabilize or stabilize the phenoxyl radical state.[6] As expected, a negligible biotin-labeling signal was detected via BNP and BMP, which was rather diffusive compared to BP in [W41F]APX-NES- or HRP-TM-expressing cells (Figure 2a).

Through density functional theory (DFT) computations, Tian and colleagues recently suggested that the bond dissociation energy (BDE) of O−H and N−H bonds within probes and the reaction barrier energy of probes with the tyrosine radical result in changes of APEX labeling efficiency.[12] In this model, low BDE and low reaction barrier energy are correlated with radical generation from the substrate and favorable radical coupling on the tyrosine residue, respectively. As model compounds, they synthesized BP5 (9) and BN2 (10): the BDE (O−H) of BP5 is lower than BDE of BP while BDE of BN2 is higher than that of BP (Figure 2b). From further calculation, BN2 was shown to have the lowest reaction barrier with tyrosine in its radical state while BP5 has the highest reaction barrier. As expected, BP5 shows a rather diffusive labeling relative to BP due to lesser reactivity with proteins, while BN2 exhibits more restricted labeling with high reactivity toward proteins (Figure 2b). The cytosolic ILK protein complex was used as a model system to test BP5 and BN2 labeling specificity using APEX2-ILK as a bait protein. All subunits of the ILK complex (e.g., ILK−PINCH-PARVIN-RSU1) were identified only by BN2, which suggests that BN2 labeling has a more precise and shorter labeling radius compared to BP and BP5.

Recent studies have shown that APEX can label biomolecules such as RNA,[13,37,38] DNA,[13] in addition to proteins. In 2019, Ting and colleagues described the APEX-seq method which enables local RNA mapping using APEX2. Using the reactivity of BP radicals to the proximal guanosine residues of local RNAs, the subcellular transcriptome, including nuclear subdomains, cytoplasm, the mitochondrial membrane, and ER cytosolic membrane (ERM), were characterized via sequencing of streptavidin bead-enriched RNA molecules after APEX labeling.[37]

To enhance RNA labeling coverage, Zou and colleagues developed biotin-phenol derivatives, including biotin-aniline (Btn-An, 11) and biotin-naphthylamine (Btn-Nap, same as 10).[13] Btn-An and Btn-Nap exhibited the strongest signals for RNA and DNA labeling, respectively, while BP was most efficient for protein (Figure 2c). In this assay, biotin-4-hydroxy-benzamide (Btn-4HB, 12) also showed promising reactivity for DNA labeling, as there was no reactivity with protein or RNA. They also confirmed that Btn-An dominantly reacted with guanosine so that labeling efficiency was highly reduced with guanosine-free oligonucleotides. Using Btn-An, they successfully characterized the mitochondrial matrix transcriptome with mitochondrial-targeted APEX2.[13] Notably, Btn-An was also utilized in a study on the confirmation of glycan-conjugated RNAs (glycoRNAs) which are localized on the cell surface and interact with sialic acid binding-immunoglobulin lectin-type (Siglec) receptor family protein (Figure 2d).[39]

■ MASS ANALYSIS OF LABELED SITES

Although PL is a powerful tool for protein labeling in live cells, most current works using PL utilize conventional mass analysis which detects the nonbiotinylated peptides of streptavidin bead-enriched proteins after APEX or BioID/TurboID labeling. This method can misidentify nonbiotinylated proteins as true positive findings (biotinylated proteins) following coenrichment with biotinylated proteins. Therefore, we developed a direct mass analysis workflow for biotinylated peptide detection via BioID (Spot-BioID)[2] or APEX (Spot-ID)[1] (Figure 3a).

First, we established Spot-BioID method and applied it for mapping the rapamycin-induced interactome of the FK506-rapamycin binding (FRB) domain within mammalian target of rapamycin (mTOR).[2] Since FRB has binding affinity for FKBP12 in the presence of rapamycin,[40] we expected to see FKBP12 among the rapamycin-dependent interaction partners of FRB-BioID. Surprisingly, in our mass analysis via Spot-BioID workflow, we observed that three lysine residues (K80, K86, and K89) of FKBP25 were the biotinylated by FRB-BioID only under rapamycin treatment (Figure 3b). Based on this finding, we further obtained the FKBP25-rapamycin-FRB ternary complex crystal structure to confirm the interaction (Figure 3b).

We also employed the Spot-BioID method for mapping mitochondria outer membrane (OMM) anchoring proteins. From the mass analysis of TOM20-BioID-biotinylated peptides, we identified that K46 and K221 of exonuclease 3′-5′ domain containing 2 (EXD2) were reproducibly biotinylated.[41] This result was not in line with previous findings on EXD2 in the nucleus[42] and mitochondrial matrix.[43] Therefore, we confirmed the subcellular localization of EXD2 via APEX-EM imaging which utilizes 3,3′-diaminobenzidine staining of APEX in the fixed sample.[41] We identified the hydrophobic N-terminus of EXD2 (1−37 aa) as an OMM-specific signal-anchor transmembrane domain for EXD2 localization to the OMM.[41] Moreover, K46 and K221 of EXD2 were biotinylated by cytosol-facing Tom20-BioID, which indicated that the soluble domain of EXD2 (38−621 aa) faces the cytoplasm. We proposed the membrane topology of EXD2 based on EM imaging and Spot-BioID LC-MS/MS results (Figure 3c). Furthermore, we successfully obtained the dimeric crystal structure of its exonuclease domain, which indicates that EXD2 forms a dimer at the cytosolic face of mitochondria.[41] Nevertheless, the molecular function of EXD2 and its nucleic acid substrates at the OMM remain unclear, and we are currently exploring these models.

In the original Spot-BioID workflow,[2,41] we first carried out "on-bead digestion", which enriched biotinylated proteins on streptavidin beads, performing trypsin digestion later. Since streptavidin can be digested by trypsin in this "on-bead" digestion protocol, we optimized a protocol for "in-solution" digestion. After biotinylation, cells were lysed via ultrasonication for nucleic acid fragmentation, and free biotin was eliminated through size-exclusion filtration or acetone precipitation. Reduction and alkylation were performed for total proteins, followed by trypsin digestion overnight. The "in-solution" trypsin digestion allows SA enrichment at the peptide level that can cover more biotinylated peptides.

Based on this modified digestion and enrichment protocol, we conducted local proteome mapping of mitochondria-associated ER membranes (MAMs) through our own designed Split-BioID system, dubbed Contact-ID, based on the B-factor of the crystal structure of BirA.[3] Since each split fragment (B1 and B2) of Contact-ID has no biotinylating activity, we expected that MAM-localized proteins can be biotinylated if the split fragment of BioID is complemented in enforced interacting spaces at the MAM. For this purpose, we prepared two constructs: an N-fragment of BioID (B1, 1−78 aa)-Sec61B for targeting the ER
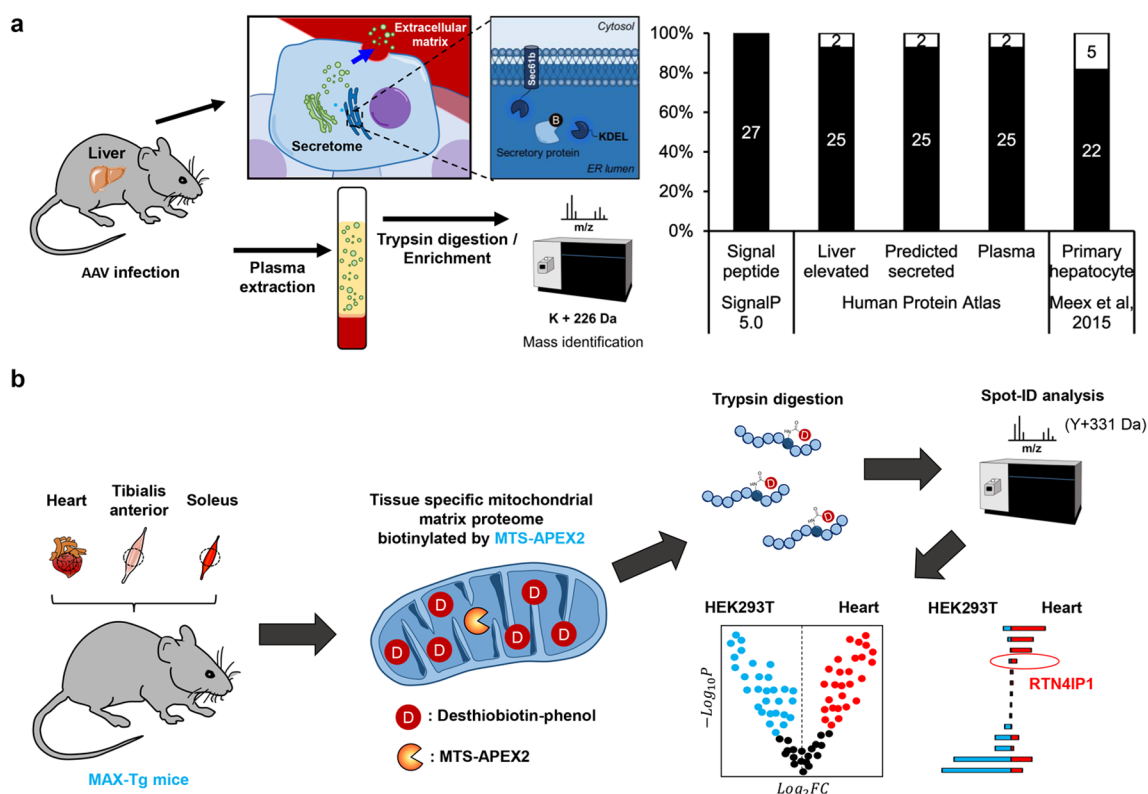
Figure 4. In vivo proximity labeling mice models. (a) Workflow of the in vivo Spot-TurboID to characterize the mouse liver secretome. Specificity of identified biotinylated proteins was analyzed using SignalP 5.0, Human Protein Atlas, and LC-MS/MS results from primary hepatocytes in literature. (b) Workflow of the ex vivo Spot-ID for mitochondrial matrix proteome mapping in various tissues. High RTN4IP1 expression was detected in the mouse heart compared to HEK293T cells.

membrane and a Tom20-C-fragment of BioID (B2, 79−321 aa) for targeting the OMM. We observed that these Contact-ID constructs generated biotinylated proteins at the contact sites of mitochondria and ER. The proteins biotinylated by Contact-ID were analyzed via a modified Spot-BioID workflow, and we identified 115 MAM-specific proteins dominantly annotated with ERM and OMM[3] (Figure 3d). Eighty-five out of 115 proteins had one or more transmembrane (TM) domains, the membrane topology of which was determined via labeling sites. FKBP8, one of the identified OMM proteins, positively regulates contact and calcium transport between the ER and mitochondria.

Direct mass analysis of the APEX-labeled site can also reveal the membrane topology of labeled membrane proteins which is conducive to understanding their functions at the membrane. Using DBP that can cover more APEX2-modified peptides (Figure 1b), we successfully identified the membrane topology of 135 inner-mitochondrial membrane (IMM) proteins via direct mass analysis of the labeled peptides, dubbed Spot-ID.[1] In this study, two APEX2 constructs, matrix-APEX2 and ScoI-APEX2 targeting the intermembrane space of mitochondria (IMS) was utilized. Because DBP radicals cannot go across the IMM, matrix- and ScoI-APEX2 exclusively labels matrix- and IMS-facing tyrosine residues of the IMM proteins, respectively (Figure 3e). From these results, we identified the topologies of 77 IMM proteins, which have not been fully characterized, and confirmed 58 IMM protein topologies.[1] In addition, the modified peptides of several bona fide IMS-side IMM proteins, such as NDUFB10, an IMS-side subunit of OXPHOS complex I,[44] were exclusively detected by IMS-APEX2 and not by matrix-

APEX2, while NDUFB10 was identified as mitochondrial matrix proteins via an indirect PL-ID workflow,[6] possibly due to the strong protein−protein interaction with biotinylated proteins on the matrix side. We also confirmed that NDUFB10 was not biotinylated by matrix-APEX2 in biochemical assay.[1] Our results demonstrated the value of direct mass detection of PL-modification site is essential for obtaining a clear picture of the spatial proteomic landscape via PL. It is noteworthy that this approach can be used for modification of other chemical probe for APEX (e.g., alkyn-phenol).[10]

■ IN VIVO APPLICATION OF PL

Accumulating evidence shows that proteomic information obtained from cultured mammalian cells may not accurately reflect the tissue of origin proteome. Tissue-specific expression databases (e.g., human protein atlas,[45] G-tex[46]) are valuable resources providing insights into the tissue-specific function of proteins; however, these databases cannot provide the spatial distribution of expressed proteins in each tissue. Recently, PL has been utilized in in vivo models to provide additional spatial information for tissue-expressed proteins in fruit flies,[47] *C. elegans*,[35] and mice.[48−52] In mice, BioID was used for mapping the inhibitory postsynapse[48] and nascent synapses[49] while split-TurboID was employed for astrocyte-synapse contact sites.[50] APEX was also used for mapping tissue-specific nuclear proteome within the mouse striatum.[52]

In these in vivo PL studies, Spot-ID (APEX2) or Spot-BioID (BioID/TurboID) methods are essential for the mass analysis of proximity-labeled tissue samples, as strong endogenous biotinylated proteins are present in tissue samples, including
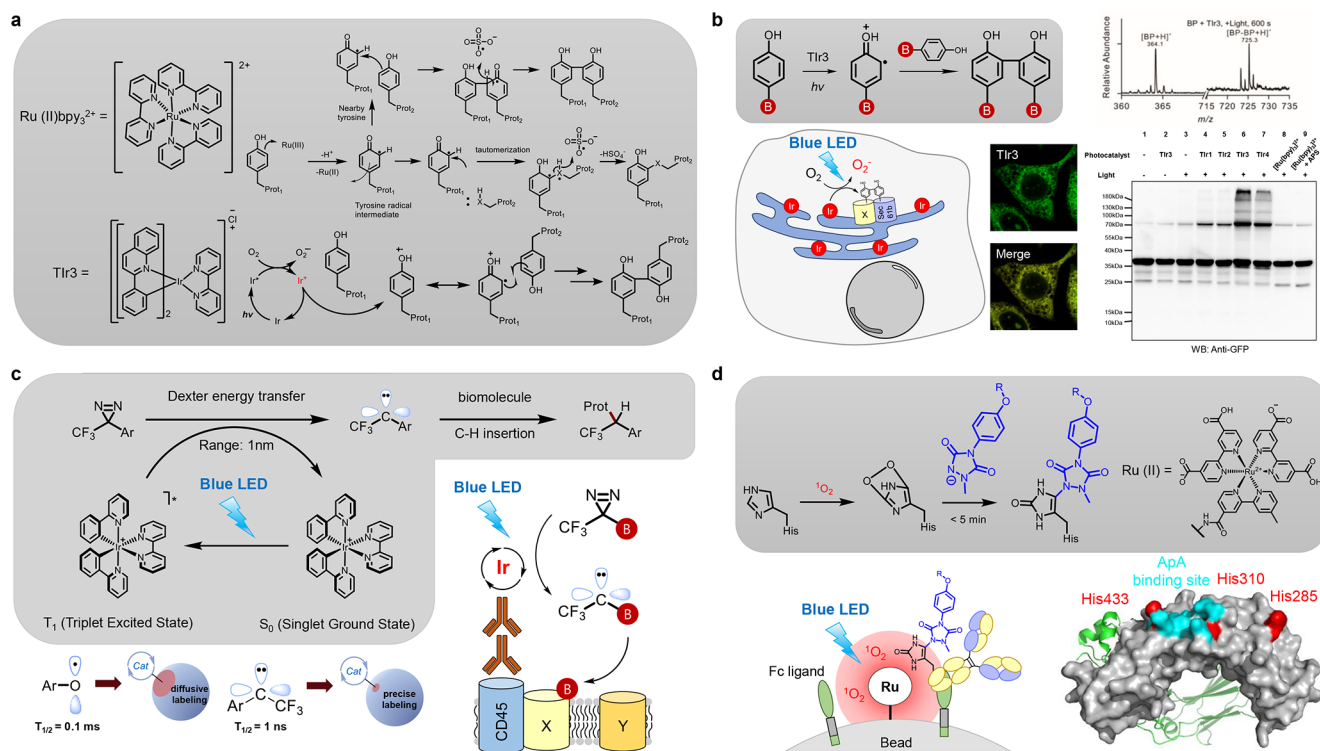
Figure 5. Photocatalyst-mediated proximity labeling. (a) Proposed mechanism of protein–protein crosslinking by the ruthenium and iridium complex. (b) Dimerization of BP by TIr3 was detected via MALDI-TOF. Western blotting results of Sec61B-GFP, which was photo-crosslinked by TIr3 targeting to the ER. Reprinted with permission from ref 55. Copyright 2016 American Chemical Society. (c) PL by the iridium complex on the Jurkat cell membrane. (d) PL of histidine residues on the trastuzumab antibody was performed via MAUra on Fc ligand-conjugated beads.

the liver or brain.[33] We recently employed the Spot-BioID workflow to analyze tissue-specific secretory protein (*i*SLET) expression in mice.[51] Since classically secreted proteins are translated at the ER lumen, we expect that the ER-anchored TurboID can biotinylate these. Then, we used the Sec61B-TurboID for anchoring to the ER membrane and facing to the lumen. We found that Sec61B-TurboID remained at the ER, while TurboID with the ER retention signal (KDEL) can be eluted to the extracellular matrix under ER stress. Sec61B-TurboID was expressed in mouse livers via adenovirus transfection, followed by treatment with biotin. Plasma was then extracted from blood, followed by trypsin digestion. Biotinylated peptides were analyzed after SA enrichment, and around 50 biotinylated proteins were identified as secretory proteins.[51] Biotinylated proteins by Sec61B-TurboID in the mouse liver showed a completely different pattern to those from a liver-derived cell line (i.e., HepG2). This result highlights the importance of in vivo proteomics (Figure 4a).

We also developed matrix-APEX transgenic mice (MAX-Tg mice) for in situ profiling of the mitochondrial matrix proteome in various tissues (Figure 4b). After sacrifice of the mice, heart, tibialis anterior (TA), and soleus muscle tissue were labeled with DBP and H_2O_2. Through the Spot-ID analysis, we identified 200, 248, and 251 DBP-labeled proteins in the heart, TA, and soleus tissue, respectively. A significant fraction of the proteins (>74%) were annotated as mitochondrial proteins, and most (>88%) localized to the matrix. Among these, reticulon 4 interacting protein 1 (RTN4IP1)/OPA10 was reproducibly enriched in the heart and soleus tissue.[53] From the structural and metabolomics analysis, we identified RTN4IP1/OPA10 as associated with the biosynthesis of coenzyme Q which is

essential for energy production and antioxidant function in mitochondrial matrix of muscle tissues. Using MAX-Tg mice, we expect to determine various unknown aspects of mitochondrial biology in differentiated tissues that cannot be explored using immortalized cell lines.

As PL can reveal tissue-specific localized proteomic information in live animal models, which cannot be achieved by conventional methods, we expect that in vivo PL has a potential to be widely employed in various animal studies including studies on disease models. However, there are several aspects that should be considered or to be investigated when using the current PL tool for in vivo studies. In case of APEX, the addition of exogenous hydrogen peroxide (H_2O_2) is required for the peroxidase reaction. As H_2O_2 induces cellular toxicity from the oxidation of cysteine and other amino acids,[54] APEX labeling in mouse model should be performed after sacrificing the mice. Exogenous addition of biotin is required for in vivo BioID or TurboID experiments[48−51] and excess biotin may cause low or negligible toxicity because biotin is a vitamin (i.e., vitamin B_7). However, possible toxicity of depletion of endogenous biotin pools by the expression of TurboID in live model[20] or possible toxicity from the accumulation of in vivo biotinylated proteins overnight should be examined in future studies.

PHOTOCATALYST-MEDIATED PL

The concepts of PL by a photocatalyst instead of enzymes were recently reported by us and others. Ir[55,56] and Ru[57,58] complex have been utilized for the generation of reactive chemical species via energy transfer[56] or electron transfer[55,57] induced by visible light. A mechanism of phenoxyl radical generation by the ruthenium(II) bipyridine complex (Rubpy) was proposed by
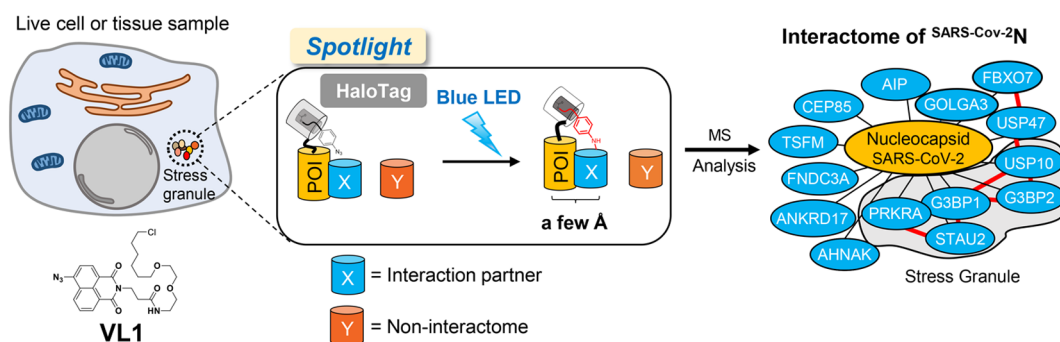
Figure 6. Proximity crosslinking method for interactome mapping. Scheme of the proximity crosslinking method (Spotlight) using photo-crosslinking ligand (VL1). Host interactome of N protein of SARS-CoV-2 was identified by Spotlight.

the Kodadek group[57] earlier. Although this method cannot be utilized in a live cell experiment because the exogenous addition of ammonium persulfate (APS) is required to reduce the oxidized Ru(III) complex (Figure 5a), it is still used for inducing protein photo-crosslinking in test tube reactions[57,59] and has also motivated scientists, including our group, to develop improved methods. In 2016, we reported an efficient tyrosine-tyrosine crosslinking reaction induced by the photoactivated iridium(III) complex using oxygen as an electron acceptor (Figure 5a).[55] Since the Ir complex has a suitable lowest unoccupied molecular orbital (LUMO) energy level to transfer an electron to oxygen, superoxide radicals ($O_2^{•-}$) can be generated efficiently via light irradiation. The oxidized Ir complex can then extract an electron from the proximal phenol moiety. We confirmed BP radical generation by the light-activated iridium dye through mass analysis of BP dimer formation without APS (Figure 5b). We also observed this photocatalytic coupling reaction in live cells. Since our Ir complex is targeted to the ER membrane, we validated the photocatalytic crosslinked product of the ER-targeted protein (i.e., Sec61B-GFP) in Ir complex-treated cells (Figure 5b).

In 2020, MacMillan and colleagues utilized the Ir complex for the photocatalytic generation of carbene from diazirine via dexter energy transfer. As the half-life of carbene[60] is estimated to be around 1 ns, much shorter than for the phenoxyl radical (~0.1 ms),[61] PL by the photoactivated Ir catalyst (termed Micromap) was proposed to have a shorter labeling radius than enzyme-mediated labeling.[56] Ir complex-conjugated antibodies were utilized to map the specific protein complexes on the cell surface, and biotin-conjugated diazirine was used as a biotinylating reagent by the Ir complex. Using this method, the interactomes of CD45, CD47, and CD29 were identified via LC-MS/MS analysis (Figure 5c).[56]

In 2021, Nakamura and colleagues reported another interesting type of photocatalytic PL using 1-methyl-4-arylurazole (MAUra). They found that the Ru complex generates singlet oxygen ($^1O_2$) which oxidizes proximal histidine residues to electrophilic oxidized histidine. After this reaction, nucleophilic MAUra can be specifically conjugated to the oxidized histidine and modified histidine residues were detected via LC-MS/MS analysis. This photocatalytic PL method was utilized for the specific modification of antibodies such as anti-HER2 antibody on Ru-complex immobilized beads with the antibody-binding Fc ligand (Figure 5d).[58]

Since several other chemical dyes (e.g., Rose Bengal[58]) or fluorescent proteins (e.g., miniSOG[62]) can generate singlet oxygen, which may oxidize local histidine residues, we expect

that MAUra can be a useful probe for the identification of proximal proteins via this photocatalytic approach. In addition, nucleic acid labeling by organic or genetically encoded photosensitizers using propargyl amine (PA) has been developed.[63−66] It is expected that PA can be conjugated to the oxidized base products of the nucleic acids by proximal photocatalysis reactions.[64,65]

■ CURRENT CHALLENGES AND OUTLOOK

PL tools (e.g., APEX or BioID/TurboID) have enabled successful local proteome mapping at the subcompartmental level. Although we and others have performed interactome mapping using APEX[1,6,10,28,35] or BioID,[2,3] two issues should be considered. First is the diffusive character of reactive species. APEX and BioID/TurboID can label not only physically interacting proteins within a few angstroms (Å) but also nearby proteins. Other PL approaches based on the diffusive reactive species, such as carbene species (Micromap[56]) or the protein-conjugated AMP ester (Pup-IT[67] or Neddylator[68]), were proposed to have an optimized labeling radius for interactome mapping which requires further comparative studies with other PL tools in the future. To overcome diffusive labeling, our lab recently developed a photoactivable proximity "crosslinking" tool (Spotlight), which utilizes HaloTag, and its visible light activable photo-crosslinking ligand (VL1).[69] We successfully revealed the host interactome of the nucleocapsid protein of SARS-CoV-2 (Figure 6).

Second, the expression of a PL-conjugated protein of interest (POI) should be controlled to endogenous levels for interactome mapping, as an overexpressed PL-POI can label proteins in the nonphysiological context. To this end, knock-in of the PL enzyme to the endogenous gene of interest (GOI) can be performed using CRISPR-Cas9.[70] However, it should be confirmed that the GOI function is not compromised by the knock-in of PL enzymes. To overcome this issue, antibody targeting of the PL enzyme in the fixed and permeabilized sample might be conducive to mapping the physiological interactome at endogenous levels when a good primary antibody is available. This antibody-based PL approach yielded successful results in the identification of interacting proteins[67] and the DNA-binding region[71] of POIs.

Our studies on the analysis of biotinylated proteins revealed that direct identification of the labeled sites (i.e., Spot-ID, Spot-BioID) provide the most accurate spatial proteomic information. We expect similar progress to be made for biotinylated nucleic acid analysis via PL as the current analysis reflects nucleic acids enriched on beads and may contain some nonbiotinylated

artifacts complexed with biotinylated nucleic acid strands during the lysis and enrichment steps. Direct detection of the PL modification site on the nucleic acid or other molecules can provide a clearer view of the spatial distribution of those molecules in live cells.

In addition, we expect that more efficient chemical probes for the PL of nucleic acids or other biomolecules will be developed in the future. As biotin-aniline exhibited higher activity for RNA labeling,[13,39] we believe that APEX probes for other nucleotides or metabolites can be developed via a rational design[12] or a chemical screening approach.[13] We also expect that other kinds of modifying enzymes can be also utilized as PL tools for specific biomolecules. It is also noticeable that chemistry-oriented PL has been recently developed through the use of photocatalysts.[72] Since chemical probe development for the photocatalyst might allow for greater probe flexibility than for enzymes, we expect photocatalyst-based PL tool development with genetically encoded fashion to be a focus in the coming decade.

■ AUTHOR INFORMATION

Corresponding Author

Hyun-Woo Rhee − *Department of Chemistry, Seoul National University, Seoul 08826, Korea;* ● orcid.org/0000-0002-3817-3455; Email: rheehw@snu.ac.kr

Author

Myeong-Gyun Kang − *Department of Chemistry, Seoul National University, Seoul 08826, Korea*

Complete contact information is available at:
https://pubs.acs.org/10.1021/acs.accounts.2c00061

Notes

The authors declare no competing financial interest.

Biographies

Myeong-Gyun Kang gained his Ph.D. degree in chemical biology at Ulsan National Institute of Science and Technology (UNIST), Korea. He is currently a postdoctoral researcher in the laboratory of Prof. Hyun-Woo Rhee at Seoul National University (SNU), Korea. His current research focuses on the construction of sub-mitochondrial proteome map using advanced proximity labeling tools.

Hyun-Woo Rhee received his Ph.D. in organic chemistry at Seoul National University (SNU), Korea. He is currently an Associate Professor at the Department of Chemistry of SNU, Korea. His current research focuses on the development of proximity labeling tools and spatial mitochondrial biology.

■ ACKNOWLEDGMENTS

■ REFERENCES

(1) Lee, S. Y.; Kang, M. G.; Shin, S.; Kwak, C.; Kwon, T.; Seo, J. K.; Kim, J. S.; Rhee, H. W. Architecture Mapping of the Inner Mitochondrial Membrane Proteome by Chemical Tools in Live Cells. *J. Am. Chem. Soc.* **2017**, *139*, 3651−3662.

(2) Lee, S. Y.; Lee, H.; Lee, H. K.; Lee, S. W.; Ha, S. C.; Kwon, T.; Seo, J. K.; Lee, C.; Rhee, H. W. Proximity-Directed Labeling Reveals a New Rapamycin-Induced Heterodimer of FKBP25 and FRB in Live Cells. *ACS Cent Sci.* **2016**, *2*, 506−516.

(3) Kwak, C.; Shin, S.; Park, J. S.; Jung, M.; Nhung, T. T. M.; Kang, M. G.; Lee, C.; Kwon, T. H.; Park, S. K.; Mun, J. Y.; Kim, J. S.; Rhee, H. W. Contact-ID, a tool for profiling organelle contact sites, reveals regulatory proteins of mitochondrial-associated membrane formation. *Proc. Natl. Acad. Sci. U. S. A.* **2020**, *117*, 12109.

(4) Choi, C. R.; Rhee, H. W. Proximity labeling: an enzymatic tool for spatial biology. *Trends Biotechnol.* **2022**, *40*, 145.

(5) Martell, J. D.; Deerinck, T. J.; Sancak, Y.; Poulos, T. L.; Mootha, V. K.; Sosinsky, G. E.; Ellisman, M. H.; Ting, A. Y. Engineered ascorbate peroxidase as a genetically encoded reporter for electron microscopy. *Nat. Biotechnol.* **2012**, *30*, 1143−1148.

(6) Rhee, H. W.; Zou, P.; Udeshi, N. D.; Martell, J. D.; Mootha, V. K.; Carr, S. A.; Ting, A. Y. Proteomic mapping of mitochondria in living cells via spatially restricted enzymatic tagging. *Science* **2013**, *339*, 1328−1331.

(7) Bendayan, M. Worth its weight in gold. *Science* **2001**, *291*, 1363−1365.

(8) Lam, S. S.; Martell, J. D.; Kamer, K. J.; Deerinck, T. J.; Ellisman, M. H.; Mootha, V. K.; Ting, A. Y. Directed evolution of APEX2 for electron microscopy and proximity labeling. *Nat. Methods* **2015**, *12*, 51−54.

(9) Sung, G.; Lee, S. Y.; Kang, M. G.; Kim, K. L.; An, J.; Sim, J.; Kim, S.; Kim, S.; Ko, J.; Rhee, H. W.; Park, K. M.; Kim, K. Supra-blot: an accurate and reliable assay for detecting target proteins with a synthetic host molecule-enzyme hybrid. *Chem. Commun. (Camb)* **2020**, *56*, 1549−1552.

(10) Li, Y.; Tian, C.; Liu, K.; Zhou, Y.; Yang, J.; Zou, P. A Clickable APEX Probe for Proximity-Dependent Proteomic Profiling in Yeast. *Cell Chem. Biol.* **2020**, *27*, 858−865.

(11) Loh, K. H.; Stawski, P. S.; Draycott, A. S.; Udeshi, N. D.; Lehrman, E. K.; Wilton, D. K.; Svinkina, T.; Deerinck, T. J.; Ellisman, M. H.; Stevens, B.; Carr, S. A.; Ting, A. Y. Proteomic Analysis of Unbounded Cellular Compartments: Synaptic Clefts. *Cell* **2016**, *166*, 1295−1307.

(12) Ke, M.; Yuan, X.; He, A.; Yu, P.; Chen, W.; Shi, Y.; Hunter, T.; Zou, P.; Tian, R. Spatiotemporal profiling of cytosolic signaling complexes in living cells by selective proximity proteomics. *Nat. Commun.* **2021**, *12*, 71.

(13) Zhou, Y.; Wang, G.; Wang, P.; Li, Z.; Yue, T.; Wang, J.; Zou, P. Expanding APEX2 Substrates for Proximity-Dependent Labeling of Nucleic Acids and Proteins in Living Cells. *Angew. Chem., Int. Ed. Engl.* **2019**, *58*, 11763−11767.

(14) Sharp, K. H.; Moody, P. C.; Brown, K. A.; Raven, E. L. Crystal structure of the ascorbate peroxidase-salicylhydroxamic acid complex. *Biochemistry* **2004**, *43*, 8644−8651.

(15) Kotani, N.; Gu, J.; Isaji, T.; Udaka, K.; Taniguchi, N.; Honke, K. Biochemical visualization of cell surface molecular clustering in living cells. *Proc. Natl. Acad. Sci. U. S. A.* **2008**, *105*, 7405−7409.

(16) Roux, K. J.; Kim, D. I.; Raida, M.; Burke, B. A promiscuous biotin ligase fusion protein identifies proximal and interacting proteins in mammalian cells. *J. Cell Biol.* **2012**, *196*, 801−810.

(17) Wood, Z. A.; Weaver, L. H.; Brown, P. H.; Beckett, D.; Matthews, B. W. Co-repressor induced order and biotin repressor dimerization: a case for divergent followed by convergent evolution. *J. Mol. Biol.* **2006**, *357*, 509−523.

(18) Weaver, L. H.; Kwon, K.; Beckett, D.; Matthews, B. W. Corepressor-induced organization and assembly of the biotin repressor: a model for allosteric activation of a transcriptional regulator. *Proc. Natl. Acad. Sci. U. S. A.* **2001**, *98*, 6045−6050.

(19) Choi-Rhee, E.; Schulman, H.; Cronan, J. E. Promiscuous protein biotinylation by Escherichia coli biotin protein ligase. *Protein Sci.* **2004**, *13*, 3043−3050.

(20) Branon, T. C.; Bosch, J. A.; Sanchez, A. D.; Udeshi, N. D.; Svinkina, T.; Carr, S. A.; Feldman, J. L.; Perrimon, N.; Ting, A. Y. Efficient proximity labeling in living cells and organisms with TurboID. *Nat. Biotechnol.* **2018**, *36*, 880−887.

(21) Demoss, J. A.; Genuth, S. M.; Novelli, G. D. The Enzymatic Activation of Amino Acids Via Their Acyl-Adenylate Derivatives. *Proc. Natl. Acad. Sci. U. S. A.* **1956**, *42*, 325−332.

(22) Hung, V.; Udeshi, N. D.; Lam, S. S.; Loh, K. H.; Cox, K. J.; Pedram, K.; Carr, S. A.; Ting, A. Y. Spatially resolved proteomic mapping in living cells with the engineered peroxidase APEX2. *Nat. Protoc* **2016**, *11*, 456−475.

(23) Tamura, T.; Hamachi, I. Chemistry for Covalent Modification of Endogenous/Native Proteins: From Test Tubes to Complex Biological Systems. *J. Am. Chem. Soc.* **2019**, *141*, 2782−2799.

(24) Rao, Y.; Wang, Z.; Luo, W.; Sheng, W.; Zhang, R.; Chai, X. Base composition is the primary factor responsible for the variation of amino acid usage in zebra finch (Taeniopygia guttata). *PLoS One* **2018**, *13*, No. e0204796.

(25) Li, H.; Frankenfield, A. M.; Houston, R.; Sekine, S.; Hao, L. Thiol-Cleavable Biotin for Chemical and Enzymatic Biotinylation and Its Application to Mitochondrial TurboID Proteomics. *J. Am. Soc. Mass Spectrom.* **2021**, *32*, 2358−2365.

(26) Slavoff, S. A.; Chen, I.; Choi, Y. A.; Ting, A. Y. Expanding the substrate tolerance of biotin ligase through exploration of enzymes from diverse species. *J. Am. Chem. Soc.* **2008**, *130*, 1160−1162.

(27) Minde, D. P.; Ramakrishna, M.; Lilley, K. S. Biotin proximity tagging favours unfolded proteins and enables the study of intrinsically disordered regions. *Commun. Biol.* **2020**, *3*, 38.

(28) Hung, V.; Zou, P.; Rhee, H. W.; Udeshi, N. D.; Cracan, V.; Svinkina, T.; Carr, S. A.; Mootha, V. K.; Ting, A. Y. Proteomic mapping of the human mitochondrial intermembrane space in live cells via ratiometric APEX tagging. *Mol. Cell* **2014**, *55*, 332−341.

(29) Jing, J.; He, L.; Sun, A.; Quintana, A.; Ding, Y.; Ma, G.; Tan, P.; Liang, X.; Zheng, X.; Chen, L.; Shi, X.; Zhang, S. L.; Zhong, L.; Huang, Y.; Dong, M. Q.; Walker, C. L.; Hogan, P. G.; Wang, Y.; Zhou, Y. Proteomic mapping of ER-PM junctions identifies STIMATE as a regulator of Ca(2)(+) influx. *Nat. Cell Biol.* **2015**, *17*, 1339−1347.

(30) Markmiller, S.; Soltanieh, S.; Server, K. L.; Mak, R.; Jin, W.; Fang, M. Y.; Luo, E. C.; Krach, F.; Yang, D.; Sen, A.; Fulzele, A.; Wozniak, J. M.; Gonzalez, D. J.; Kankel, M. W.; Gao, F. B.; Bennett, E. J.; Lecuyer, E.; Yeo, G. W. Context-Dependent and Disease-Specific Diversity in Protein Interactions within Stress Granules. *Cell* **2018**, *172*, 590−604.

(31) Paek, J.; Kalocsay, M.; Staus, D. P.; Wingler, L.; Pascolutti, R.; Paulo, J. A.; Gygi, S. P.; Kruse, A. C. Multidimensional Tracking of GPCR Signaling via Peroxidase-Catalyzed Proximity Labeling. *Cell* **2017**, *169*, 338−349.

(32) An, J.; Kim, S.; Shrinidhi, A.; Kim, J.; Banna, H.; Sung, G.; Park, K. M.; Kim, K. Purification of protein therapeutics via high-affinity supramolecular host-guest interactions. *Nat. Biomed. Eng.* **2020**, *4*, 1044−1052.

(33) Cooper, K. M.; Kennedy, S.; McConnell, S.; Kennedy, D. G.; Frigg, M. An immunohistochemical study of the distribution of biotin in tissues of pigs and chickens. *Res. Vet. Sci.* **1997**, *63*, 219−225.

(34) Chen, C. L.; Hu, Y.; Udeshi, N. D.; Lau, T. Y.; Wirtz-Peitz, F.; He, L.; Ting, A. Y.; Carr, S. A.; Perrimon, N. Proteomic mapping in live Drosophila tissues using an engineered ascorbate peroxidase. *Proc. Natl. Acad. Sci. U. S. A.* **2015**, *112*, 12093−12098.

(35) Reinke, A. W.; Mak, R.; Troemel, E. R.; Bennett, E. J. In vivo mapping of tissue-and subcellular-specific proteomes in Caenorhabditis elegans. *Sci. Adv.* **2017**, *3*, No. e1602426.

(36) Hwang, J.; Espenshade, P. J. Proximity-dependent biotin labelling in yeast using the engineered ascorbate peroxidase APEX2. *Biochem. J.* **2016**, *473*, 2463−2469.

(37) Fazal, F. M.; Han, S.; Parker, K. R.; Kaewsapsak, P.; Xu, J.; Boettiger, A. N.; Chang, H. Y.; Ting, A. Y. Atlas of Subcellular RNA Localization Revealed by APEX-Seq. *Cell* **2019**, *178*, 473−490.

(38) Padron, A.; Iwasaki, S.; Ingolia, N. T. Proximity RNA Labeling by APEX-Seq Reveals the Organization of Translation Initiation Complexes and Repressive RNA Granules. *Mol. Cell* **2019**, *75*, 875−887.

(39) Flynn, R. A.; Pedram, K.; Malaker, S. A.; Batista, P. J.; Smith, B. A. H.; Johnson, A. G.; George, B. M.; Majzoub, K.; Villalta, P. W.; Carette, J. E.; Bertozzi, C. R. Small RNAs are modified with N-glycans and displayed on the surface of living cells. *Cell* **2021**, *184*, 3109−3124.

(40) Banaszynski, L. A.; Liu, C. W.; Wandless, T. J. Characterization of the FKBP.rapamycin.FRB ternary complex. *J. Am. Chem. Soc.* **2005**, *127*, 4715−4721.

(41) Park, J.; Lee, S. Y.; Jeong, H.; Kang, M. G.; Van Haute, L.; Minczuk, M.; Seo, J. K.; Jun, Y.; Myung, K.; Rhee, H. W.; Lee, C. The structure of human EXD2 reveals a chimeric 3′ to 5′ exonuclease domain that discriminates substrates via metal coordination. *Nucleic Acids Res.* **2019**, *47*, 7078−7093.

(42) Broderick, R.; Nieminuszczy, J.; Baddock, H. T.; Deshpande, R.; Gileadi, O.; Paull, T. T.; McHugh, P. J.; Niedzwiedz, W. EXD2 promotes homologous recombination by facilitating DNA end resection. *Nat. Cell Biol.* **2016**, *18*, 271−280.

(43) Silva, J.; Aivio, S.; Knobel, P. A.; Bailey, L. J.; Casali, A.; Vinaixa, M.; Garcia-Cao, I.; Coyaud, E.; Jourdain, A. A.; Perez-Ferreros, P.; Rojas, A. M.; Antolin-Fontes, A.; Samino-Gene, S.; Raught, B.; Gonzalez-Reyes, A.; Ribas de Pouplana, L.; Doherty, A. J.; Yanes, O.; Stracker, T. H. EXD2 governs germ stem cell homeostasis and lifespan by promoting mitoribosome integrity and translation. *Nat. Cell Biol.* **2018**, *20*, 162−174.

(44) Zhu, J.; Vinothkumar, K. R.; Hirst, J. Structure of mammalian respiratory complex I. *Nature* **2016**, *536*, 354−358.

(45) Uhlen, M.; Fagerberg, L.; Hallstrom, B. M.; Lindskog, C.; Oksvold, P.; Mardinoglu, A.; Sivertsson, A.; Kampf, C.; Sjostedt, E.; Asplund, A.; Olsson, I.; Edlund, K.; Lundberg, E.; Navani, S.; Szigyarto, C. A.; Odeberg, J.; Djureinovic, D.; Takanen, J. O.; Hober, S.; Alm, T.; Edqvist, P. H.; Berling, H.; Tegel, H.; Mulder, J.; Rockberg, J.; Nilsson, P.; Schwenk, J. M.; Hamsten, M.; von Feilitzen, K.; Forsberg, M.; Persson, L.; Johansson, F.; Zwahlen, M.; von Heijne, G.; Nielsen, J.; Ponten, F. Tissue-based map of the human proteome. *Science* **2015**, *347*, 1260419.

(46) Lonsdale, J.; Thomas, J.; Salvatore, M.; et al. The Genotype-Tissue Expression (GTEx) project. *Nat. Genet.* **2013**, *45*, 580−585.

(47) Mannix, K. M.; Starble, R. M.; Kaufman, R. S.; Cooley, L. Proximity labeling reveals novel interactomes in live Drosophila tissue. *Development* **2019**, *146*.

(48) Uezu, A.; Kanak, D. J.; Bradshaw, T. W.; Soderblom, E. J.; Catavero, C. M.; Burette, A. C.; Weinberg, R. J.; Soderling, S. H. Identification of an elaborate complex mediating postsynaptic inhibition. *Science* **2016**, *353*, 1123−1129.

(49) Spence, E. F.; Dube, S.; Uezu, A.; Locke, M.; Soderblom, E. J.; Soderling, S. H. In vivo proximity proteomics of nascent synapses reveals a novel regulator of cytoskeleton-mediated synaptic maturation. *Nat. Commun.* **2019**, *10*, 386.

(50) Takano, T.; Wallace, J. T.; Baldwin, K. T.; Purkey, A. M.; Uezu, A.; Courtland, J. L.; Soderblom, E. J.; Shimogori, T.; Maness, P. F.; Eroglu, C.; Soderling, S. H. Chemico-genetic discovery of astrocytic control of inhibition in vivo. *Nature* **2020**, *588*, 296−302.

(51) Kim, K. E.; Park, I.; Kim, J.; Kang, M. G.; Choi, W. G.; Shin, H.; Kim, J. S.; Rhee, H. W.; Suh, J. M. Dynamic tracking and identification of tissue-specific secretory proteins in the circulation of live mice. *Nat. Commun.* **2021**, *12*, 5204.

(52) Dumrongprechachan, V.; Salisbury, R. B.; Soto, G.; Kumar, M.; MacDonald, M. L.; Kozorovitskiy, Y. Cell-type and subcellular compartment-specific APEX2 proximity labeling reveals activity-dependent nuclear proteome dynamics in the striatum. *Nat. Commun.* **2021**, *12*, 4855.

(53) Park, I.; Kim, K.-e.; Kim, J.; Bae, S.; Jung, M.; Choi, J.; Kwak, C.; Kang, M.-G.; Yoo, C.-M.; Mun, J. Y.; Liu, K.-H.; Kim, J.-S.; Suh, J. M.; Rhee, H.-W. *Biorxiv (Preprint server)*, **2021**, DOI: 10.1101/2021.10.14.464368.

(54) Finnegan, M.; Linley, E.; Denyer, S. P.; McDonnell, G.; Simons, C.; Maillard, J. Y. Mode of action of hydrogen peroxide and other oxidizing agents: differences between liquid and gas forms. *J. Antimicrob. Chemother.* **2010**, *65*, 2108−2115.

(55) Nam, J. S.; Kang, M. G.; Kang, J.; Park, S. Y.; Lee, S. J.; Kim, H. T.; Seo, J. K.; Kwon, O. H.; Lim, M. H.; Rhee, H. W.; Kwon, T. H. Endoplasmic Reticulum-Localized Iridium(III) Complexes as Efficient Photodynamic Therapy Agents via Protein Modifications. *J. Am. Chem. Soc.* **2016**, *138*, 10968−10977.

(56) Geri, J. B.; Oakley, J. V.; Reyes-Robles, T.; Wang, T.; McCarver, S. J.; White, C. H.; Rodriguez-Rivera, F. P.; Parker, D. L., Jr.; Hett, E. C.; Fadeyi, O. O.; Oslund, R. C.; MacMillan, D. W. C. Microenvironment mapping via Dexter energy transfer on immune cells. *Science* **2020**, *367*, 1091−1097.

(57) Fancy, D. A.; Kodadek, T. Chemistry for the analysis of protein-protein interactions: rapid and efficient cross-linking triggered by long wavelength light. *Proc. Natl. Acad. Sci. U. S. A.* **1999**, *96*, 6020−6024.

(58) Nakane, K.; Sato, S.; Niwa, T.; Tsushima, M.; Tomoshige, S.; Taguchi, H.; Ishikawa, M.; Nakamura, H. Proximity Histidine Labeling by Umpolung Strategy Using Singlet Oxygen. *J. Am. Chem. Soc.* **2021**, *143*, 7726−7731.

(59) Elvin, C. M.; Carr, A. G.; Huson, M. G.; Maxwell, J. M.; Pearson, R. D.; Vuocolo, T.; Liyou, N. E.; Wong, D. C.; Merritt, D. J.; Dixon, N. E. Synthesis and properties of crosslinked recombinant pro-resilin. *Nature* **2005**, *437*, 999−1002.

(60) Wang, J.; Kubicki, J.; Peng, H.; Platz, M. S. Influence of solvent on carbene intersystem crossing rates. *J. Am. Chem. Soc.* **2008**, *130*, 6604−6609.

(61) Folkes, L. K.; Trujillo, M.; Bartesaghi, S.; Radi, R.; Wardman, P. Kinetics of reduction of tyrosine phenoxyl radicals by glutathione. *Arch. Biochem. Biophys.* **2011**, *506*, 242−249.

(62) Shu, X.; Lev-Ram, V.; Deerinck, T. J.; Qi, Y.; Ramko, E. B.; Davidson, M. W.; Jin, Y.; Ellisman, M. H.; Tsien, R. Y. A genetically encoded tag for correlated light and electron microscopy of intact cells, tissues, and organisms. *PLoS Biol.* **2011**, *9*, No. e1001041.

(63) Li, Y.; Aggarwal, M. B.; Nguyen, K.; Ke, K.; Spitale, R. C. Assaying RNA Localization in Situ with Spatially Restricted Nucleobase Oxidation. *ACS Chem. Biol.* **2017**, *12*, 2709−2714.

(64) Wang, P.; Tang, W.; Li, Z.; Zou, Z.; Zhou, Y.; Li, R.; Xiong, T.; Wang, J.; Zou, P. Mapping spatial transcriptome with light-activated proximity-dependent RNA labeling. *Nat. Chem. Biol.* **2019**, *15*, 1110−1119.

(65) Ding, T.; Zhu, L.; Fang, Y.; Liu, Y.; Tang, W.; Zou, P. Chromophore-Assisted Proximity Labeling of DNA Reveals Chromosomal Organization in Living Cells. *Angew. Chem., Int. Ed. Engl.* **2020**, *59*, 22933−22937.

(66) Engel, K. L.; Lo, H. G.; Goering, R.; Li, Y.; Spitale, R. C.; Taliaferro, J. M. Analysis of subcellular transcriptomes by RNA proximity labeling with Halo-seq. *Nucleic Acids Res.* **2022**, *50*, No. e24.

(67) Bar, D. Z.; Atkatsh, K.; Tavarez, U.; Erdos, M. R.; Gruenbaum, Y.; Collins, F. S. Biotinylation by antibody recognition-a method for proximity labeling. *Nat. Methods* **2018**, *15*, 127−133.

(68) Hill, Z. B.; Pollock, S. B.; Zhuang, M.; Wells, J. A. Direct Proximity Tagging of Small Molecule Protein Targets Using an Engineered NEDD8 Ligase. *J. Am. Chem. Soc.* **2016**, *138*, 13123−13126.

(69) Mishra, P. K.; Kang, M.-G.; Lee, H.; Kim, S.; Choi, S.; Sharma, N.; Park, C.-M.; Ko, J.; Lee, C.; Seo, J. K.; Rhee, H.-W. A chemical tool for blue light-inducible proximity photo-crosslinking in live cells. *Chem. Sci.* **2022**, *13*, 955.

(70) Feng, W.; Liu, C.; Spinozzi, S.; Wang, L.; Evans, S. M.; Chen, J. Identifying the Cardiac Dyad Proteome In Vivo by a BioID2 Knock-In Strategy. *Circulation* **2020**, *141*, 940−942.

(71) Chen, Y.; Zhang, Y.; Wang, Y.; Zhang, L.; Brinkman, E. K.; Adam, S. A.; Goldman, R.; van Steensel, B.; Ma, J.; Belmont, A. S. Mapping 3D genome organization relative to nuclear compartments using TSA-Seq as a cytological ruler. *J. Cell Biol.* **2018**, *217*, 4025−4048.

(72) Prier, C. K.; Rankic, D. A.; MacMillan, D. W. Visible light photoredox catalysis with transition metal complexes: applications in organic synthesis. *Chem. Rev.* **2013**, *113*, 5322−5363.